

Design, Development and Experiments of a High Stroke-Precision 2DoF (Linear-Angular) Microsystem

Micky Rakotondrabe, Yassine Haddab and Philippe Lutz
Laboratoire d'Automatique de Besançon - CNRS UMR6596
Université de Franche-Comté - ENSMM
24, rue Alain Savary
25000 Besançon - France
{mrakoton,yhaddab,plutz}@ens2m.fr

Abstract—This paper presents the design, the development and the experiments on a two degrees of freedom (2DoF) microsystem. The originality of the microsystem is its ability to do angular and linear motions independently with a very high stroke and a submicrometric precision. The target performances are first presented. Afterwards the stick-slip piezoelectric microactuators that are used are presented. Then, their integration inside the microsystem is detailed. Finally, results of experiments are given.

Keywords : Micromanipulation system, angular and linear motions, piezoelectric actuator, design and development, stick-slip.

I. INTRODUCTION

To assemble and to process microproducts, especially MEMS (MicroElectroMechanical Systems), the use of conventional assembly systems leads to important difficulties because of the scale effects (adhesion forces [1] ...) and the complexity of the physics of the microworld. In order to take into account these scale effects, a complete study of the actuators, the sensors and the production methods must be done. On the other hand, microproducts production systems should have dimensions which are adapted to the one of the products. Those systems are called microfactories.

As part of a microfactory concept [2][3], a micromanipulation station is made up of two independent microsystems having each one two degrees of freedom (rotation and linear motions) (see Fig. 1). That allows the station to manipulate microparts with a high range of dimensions, from $10\mu\text{m}$ to some millimeters (2mm). The aim of this paper is the design, development and experiments of the 2DoF microsystem. The paper is organized as follow : Section II presents the wanted performances and characteristics of the microsystem. Section III details the design and development of it. The experiment results are presented in Section IV and the last section contains some discussions and perspectives.

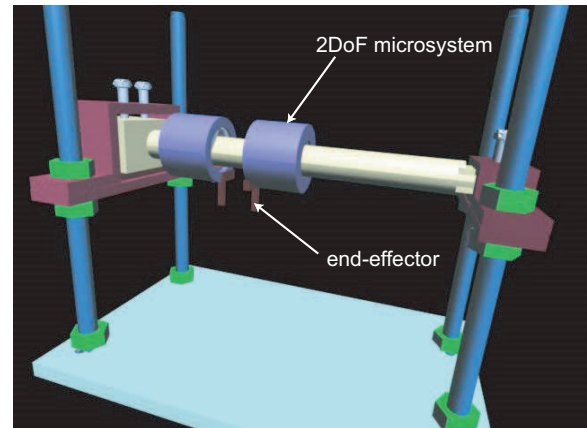


Fig. 1. Two independent microsystems having each one 2DoF (linear and angular) constitute a micromanipulation module for a station. This paper deals with one of these microsystems.

II. TARGET SYSTEM

A. Desired characteristics of the microsystem

- The microsystem has two degrees of freedom (DoF) : linear and angular motions,
- the desired precision is better than $1\mu\text{m}$,
- in each motion, a very high stroke must be possible : more than 5cm in the linear motion and 360° in the angular one,
- finally, as the microsystem is dedicated to a microfactory, it must have an adequate size. For example, if the range of the linear motion is about 5cm , the total dimensions of the microsystem and its support should be inferior to $10\text{cm} * 10\text{cm} * 10\text{cm}$.

B. Microactuators used

In order to have a large displacement, embedded actuators must be used. For example, *Stick-Slip* ([4], [5]) or *Inch-Worm* ([6], [7]) principle seems convenient. In [8], stick-slip piezoelectric based microactuator is proposed. It offers the possibility to have more DoF from only one bulk material and

it has a sub-micrometric precision. Due to its compactness and performance, this type of microactuator is used. Fig. 2 represents the principle of the actuator.

On a piezoelectric plate, two electrodes are placed on the upper face and the ground electrode on the lower face (see Fig. 2-a). When symmetric voltages are applied to the electrodes, the half part of the plate expands while the second half is compressed (see Fig. 2-b). If there is a hemispherical end-effector on the plate, its center (the point C) will have a displacement δx in the same time that a rotation ϕ will appear.

Now, let us place a slider on the end-effector (see Fig. 2-c) and always apply symmetric voltages to the electrodes. If the friction between the end-effector and the slider doesn't exceed the stiction, the slider moves on it due to δx and ϕ . If r_e is the radius of the hemisphere, this displacement will be : $\Delta x = r_e \cdot \phi + \delta x$ so that $\phi \cdot \delta x < 0$. The stickiness is obtained when the rate of the voltages is slow. However, when the voltages are abruptly removed, the accelerations of δx and ϕ are very high so that the friction will exceed the stiction and the slider doesn't move. Then, applying a sawtooth voltage signal, we obtain a high stroke of the slider motion. On the other hand, if we place the microactuator on a base, the microactuator will move along it.

According to the configuration of the electrodes, it is possible to obtain more than 1DoF from a bulk material [9]. As an example, Fig. 2-d represents a configuration that allows 2DoF for the linear motion.

III. DESIGN

In this section, we study the integration of the microactuator inside a microsystem. To maintain the radial equilibrium

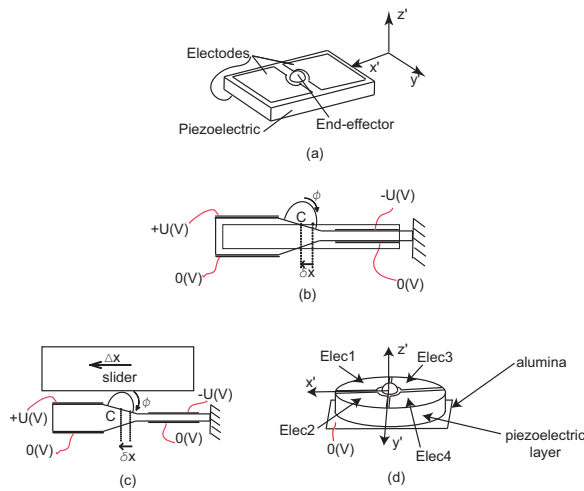


Fig. 2. Principle of the microactuator proposed in [8]. a : the microactuator. b : state when applying voltages to the electrodes. c : putting a slider on the end-effector. d : a configuration of the electrodes in order to obtain 2DoF.

of the microsystem, three contact points spread out 360° are used (see Fig. 3-a). On the other hand, to maintain the axial equilibrium, we use two contact points (see Fig. 3-b). There are then three pairs of contact point between the microsystem and the tube (spindle).

In order to obtain 2DoF of the microsystem, the microactuator used must also have 2DoF. So we use the configuration of microactuator shown in Fig. Fig. 2-d. Each end-effector will be a contact point. A pair of microactuators is then glued in a rigid plate (we use alumina Al_2O_2) in order to obtain the axial guidance (see Fig. 4-a). We use alumina because its rigidity and its dielectric coefficient ensure the transfer of the microactuators' motions to the microsystem and the electrical isolation of the lower face electrodes of the microactuators. Three plates are spread out 360° to complete the equilibrium (see Fig. 4-b) (radial equilibrium and axial equilibrium). To minimize the friction during sliding and then to avoid the overheating, we use end-effectors which are made of sapphire and an ordinary glass-tube. However, as ordinary glass-tubes have a high cylindricity defect, the microsystem may give bad performances. To resolve that, we introduce an adaptable spring in series with one of the alumina plates. By using a spring however, low frequency vibrations may appear during functioning.

On each microactuator, there are four electrodes ($Elec1 \rightarrow Elec4$) for the sawtooth signal and one electrode for the ground reference (Fig. 2-d). All the six micro-actuators (ie. the three pairs of microactuators) are supplied in parallel : all the $Elec1$ have the same potential, etc... In order to obtain linear motion, we apply a sawtooth voltage $U(t)$ to all the $Elec1$ and $Elec3$ while $-U(t)$ to all the $Elec2$ and $Elec4$. On the other hand, to obtain the angular motion, we apply a sawtooth voltage $U(t)$ to all the $Elec1$ and $Elec2$ while $-U(t)$ to all $Elec3$ and $Elec4$.

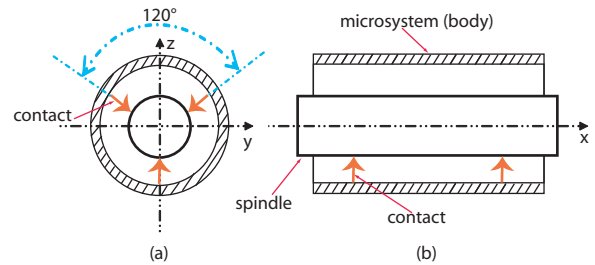


Fig. 3. Repartition of the contact points between a microsystem and the spindle (tube).

A. First design

In a previous work [10], a model of the microsystem using the previous microactuator with a hemispherical end-effector (see Fig. 4-a) has been developed. It was shown that the microsystem moves with *stick-skid* principle but not *stick – slip*. In fact, the designation *skid* was introduced because when the voltages are abruptly removed, the center of the hemisphere (point *C*) doesn't move ($\frac{d\delta x}{dt} = 0$) while the hemisphere turns ($\frac{d\phi}{dt} \neq 0$). In *slip* mode, the end-effector would slide ($\frac{d\delta x}{dt} \neq 0$ and $\frac{d\phi}{dt} = 0$). In the modelling, each phase (*stick* and *skid*) of each motion (rotation or linear motion) were developed separately. Despite the modelling, if the hemisphere is not radial in relation with the tube at rest, operating problems may appear. The difficulty to carry out this condition lead us to use a cylindrical end-effector instead of hemispherical one.

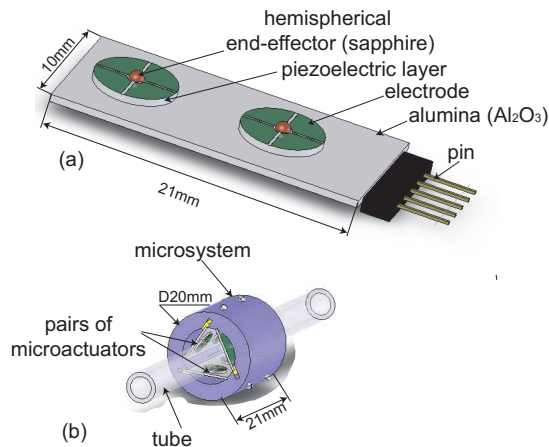


Fig. 4. Integration of the microactuators inside the microsystem. a : a pair of microactuators are used to ensure the axial guidance and equilibrium. They are glued on a plate of alumina. In this scheme, the end-effectors are hemispherical. b : three plates are shared out 360° to ensure the angular guidance and equilibrium.

B. Final design

The final design implies a cylindrical end-effector for each microactuator. The radial force \vec{N} permits each cylindrical effector to be pinned against the tube and is adjustable by screws and tilted plates (see Fig. 5-a). Another screw maintain the whole "microactuator + alumina plate + tilted plate" to be pinned against the body when the radial force adjustment is finished. The radial adaptable spring is put under the third pair of microactuators where there are neither lower tilted plate nor screw. This radial spring and the lateral one are fabricated with a thin metallic plate (see Fig. 5-b). We put its stiffness as small as possible in order to have

practically a constant force whatever the defect of the tube is. When the radial force is sufficient, the system operates in *stick-slip* mode because there is no rotation ϕ of the end-effector but only a displacement δx .

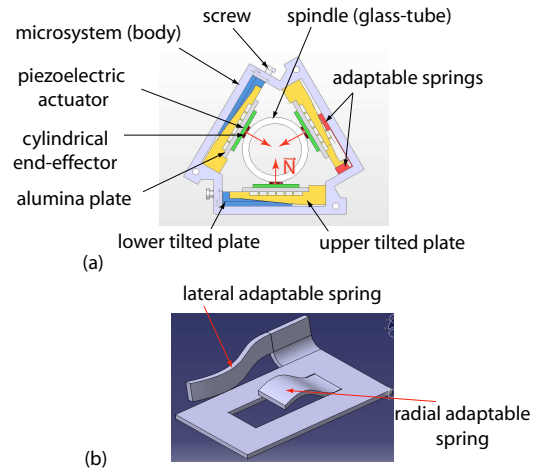


Fig. 5. a : We use cylindrical end-effectors for the microactuators. Tilted plates let us modify the radial force. The adaptable spring is put under the third tilted plates. b : the two springs are made of one thin metallic plate.

Besides the dimensions, weight is the principal criteria of the design because the torque that the microactuators can deliver to move the microsystem is very limited. The microsystem and the tilted plates are then made of aluminium because of the rigidity and the lightness that it offers. So, the load of the whole microsystem is about $100mN$. According to experiments on the microactuators done, to avoid destruction of the microactuators, the radial force must not exceed $5N$ per end-effector. Fig. 6 shows the components of the microsystem before the assembly. As the dimensions are small and the shape is complex, the body and the tilted plates were fabricated with electro-erosion technology. The adaptable spring is got by folding and shearing a thin metallic plate (*thickness* = $0.05mm$). Fig. 7 shows the microsystem tube positioned on the glass tube.

IV. EXPERIMENTS

In this section, we present the results of experiments for each motion : linear and angular. We first show the results in small displacements, ie , one step of the *stick-slip* mode. The aim is to evaluate the amplitude in each motion. Then, we will experiment the large displacement in order to evaluate the speed according to the frequency and the voltage applied.

Three sensors are used to perform the measurements. The first one is an optical sensor (from *KEYENCE*) which

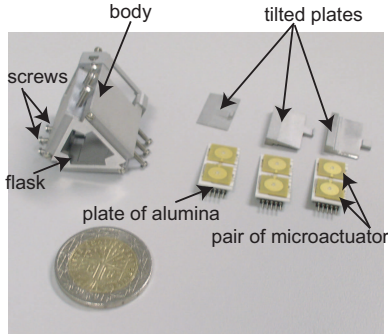


Fig. 6. The components of the microsystem before assembly.

has a $10nm$ of resolution and $30nm$ of accuracy but its working range is very limited ($\pm 200\mu m$). It is used to measure the small displacements in linear and in angular motions. In fact, we consider that $tg(\theta) = \theta = \frac{m}{R}$ where θ represents the angular displacement of the microsystem, m is the tangential displacement and R is the radius (see Fig. 8). The second sensor used is an optical sensor with a high range (from BULLIER) to measure the large displacement in linear motion. Its working range is $\pm 10mm$ and it has a resolution of $6\mu m$. In order to measure the large displacement of the angular motion, a third sensor based on capacitive micromachined inclinometer is used (MMA6263Q from FREESCALE). Due to its low weight ($< 2g$) and its small dimensions, it is easily integrated on the microsystem. According to the electronic amplifier used, its resolution can reach $0.008rad$. We notice that during all the experiments there is no indication of scratch or crack of the glass-tube due by the sapphire. On the other hand, a quick test shows that the microsystem may push a load up to $2N$ in linear motion.

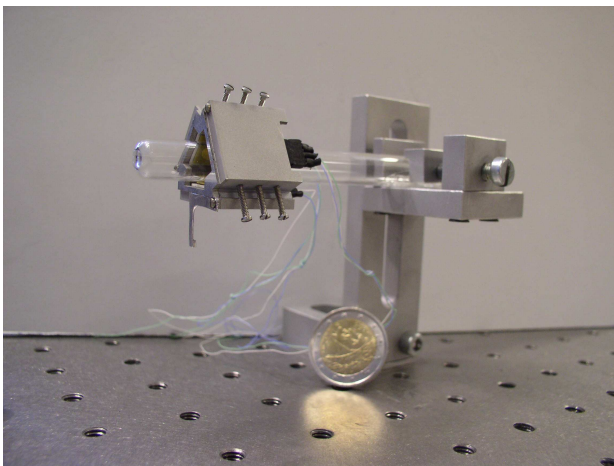


Fig. 7. Photo of the microsystem on the glass tube.

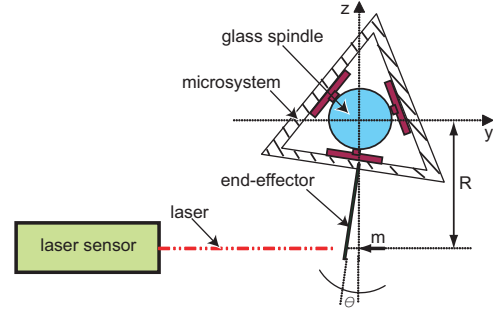


Fig. 8. We use the optical sensor for linear motion to measure the angular small displacement.

A. Step measurements

Fig. 9 shows the displacement of the microsystem in linear motion. In this experiment, we apply saw-tooth voltages with amplitude $U = \pm 150V$. On the curve, we can remark that the step is sub-micrometric and is practically constant during a large displacement. However, according to the applied frequency, it changes a little. At $100Hz$, the amplitude of a step is around $100nm$. We observe that the amplitude of the step tends towards $170nm$ when the frequency tends towards $15kHz$. We also remark the existence of vibrations during the stick. It is due to the application of the voltage step (from $+150V$ to $-150V$) on slip mode. On the other hand, the measurement of angular motion (see Fig. 10) shows that the step is nearly constant during the displacement and its amplitude is about $0.05 \cdot 10^{-4}rad$. In the two cases (linear and angular motions), the amplitudes of the steps are small enough to be compatible with our requirements.

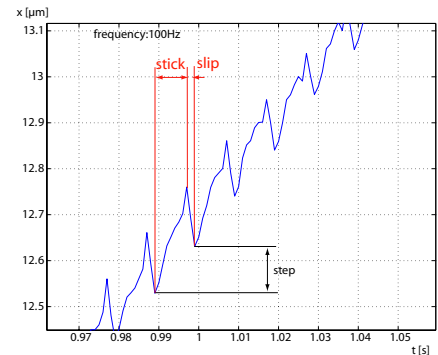


Fig. 9. Measurement of the steps in linear motion : voltage $U = 150V$ and frequency $f = 100Hz$.

B. High stroke experiments

Here, we present the speed performances of the microsystem according to different values of voltage and

frequency.

1) *Linear motion:* Our first measurements in large stroke were to check if the tube defect affects the displacement linearity of the microsystem. Fig. 11-a shows that the motion of the microsystem along the tube is linear for different frequencies when $U = 150V$. Similarly, for different voltage when $f = 10kHz$, the motion is quasi-linear along the tube (see Fig. 11-b). We conclude that the spring made for the cylindrical defect and its stiffness is well adapted.

We deduce from Fig. 12-a the speed performances according to the applied voltage. The maximal voltage supported by the microactuators is $160V$. However, between $40V$ and $60V$, dysfunctions appear. Below $40V$, the microsystem can't move. From the figure, we can assume that the speed is nearly linear vs the voltage. The spectrum of the speed is shown in Fig. 12-b. We see that at the frequencies $8.5kHz$, $14.5kHz$, $16kHz$ and $17.5kHz$, there are local minimum. In fact, these frequencies correspond to natural frequencies of the microactuator and/or the tube. The curve may be divided into two parts :

- the first part is the linear part, from $100Hz$ up to $12kHz$. Except the local minimum, this part may be interesting for closed-loop control using frequency as input.
- the second part is above $12kHz$: saturation and loss of speed appear. This means that above a certain value of frequency, the slope of the voltage is too high and the strain acceleration of the microactuator may generate a force which exceeds the stiction. Some stick phase doesn't appear during the motion.

We notice that the minimum frequency which let the microsystem move is about $0.5Hz$ for a voltage of $U = 150V$.

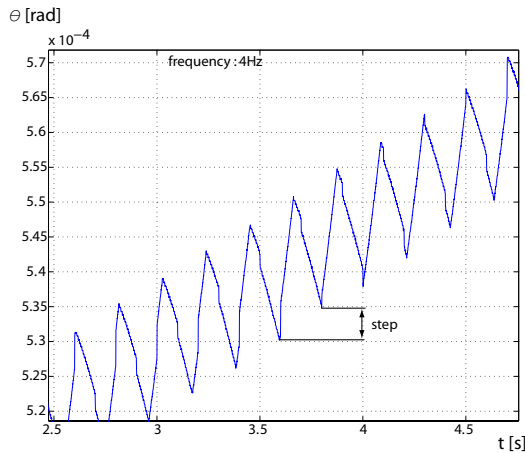


Fig. 10. Measurement of the steps in angular motion. The applied voltage is $U = 150V$ and the frequency $f = 4Hz$.

2) *Angular motion:* Fig. 13-a shows that the microsystem has a linear displacement around the glass tube even if it presents minor defect of circularity. Fig. 13-b presents the spectrum of the average speed. Similarly to linear motion, we see the diminution of the speed at about $8.5kHz$.

V. CONCLUSION

In this paper, the design and the development of a microsystem with two degrees of freedom were presented. The microsystem uses piezoelectric microactuators in stick-slip mode. The steps amplitude varies according to the frequency and the amplitude of the voltages. The maximal step value is $170nm$ in linear motion and $0.18rad$ in angular motion. These values are obtained when the frequency is about $13kHz$. At this frequency, the maximal speeds are obtained ($2.8mm/s$ in linear motion and $0.22rad/s$ in angular motion). The results obtained fulfill the requirements for the

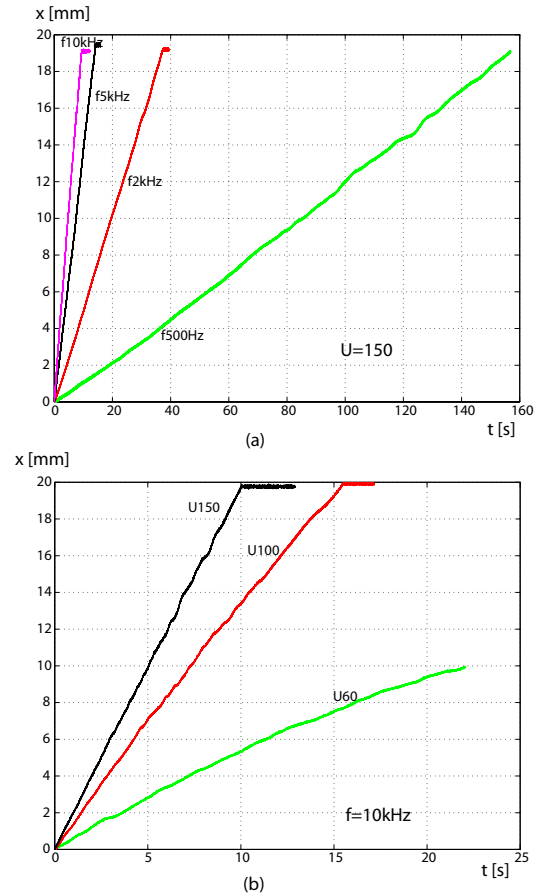


Fig. 11. The linear displacement of the microsystem along the tube is practically linear. That means that the adaptable spring compensates efficiently the defect of the tube.

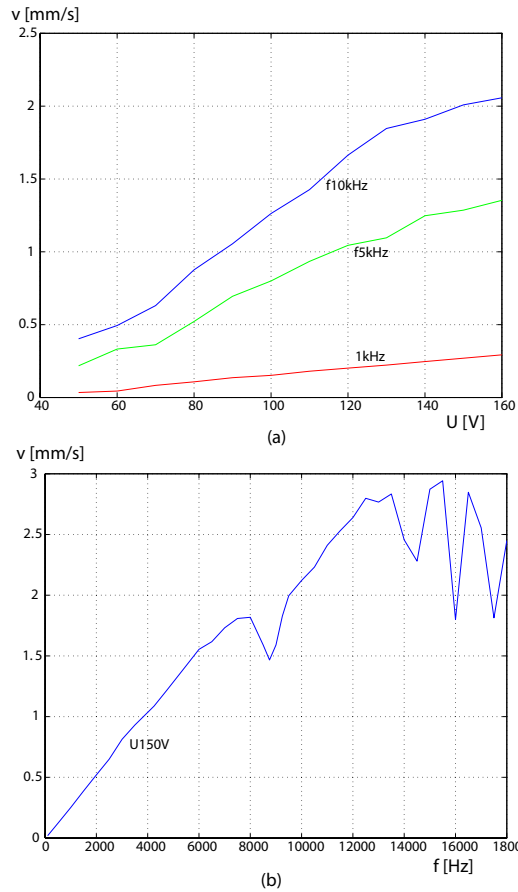


Fig. 12. Performances on speed of the microsystem in linear motion. a : speed vs voltages. b : spectrum of the speed.

system. The next work is to use two microsystems in cooperation on a tube (see Fig. 1) in order to manipulate microparts. After that, closed loop control (force and position) will be studied.

ACKNOWLEDGMENT

Particular thanks to Dr Jean-Marc Breguet and team from the 'Laboratoire des Systèmes Robotiques' of the Swiss Federal Institute of Technology Lausanne (LSRO - EPFL) for providing us the microactuators and many precious advises.

REFERENCES

- [1] R.S. Fearing, "Survey of sticking effect for micro parts handling" Proceeding of International Conference on Intelligent Robots and Systems, IROS'95, Vol.2, pp-212-227, Pittsburgh, PA, USA 1995.
- [2] M. Rakotondrabe, Y. Haddab, P. Lutz, "Modular and re-organizable micromanipulation station" Proceedings of the Workshop on Microrobotics, Journées du RTP-Microrobotique, December 2004, Lausanne, Switzerland.
- [3] E. Descouvrières, D. Geandreau, P. Lutz and F. Kieffer, "Specifications of technical information system dedicated to a re-organizable and re-configurable microfactory" 4th International Workshop on Microfactory, IWMF, China, October, 2004.

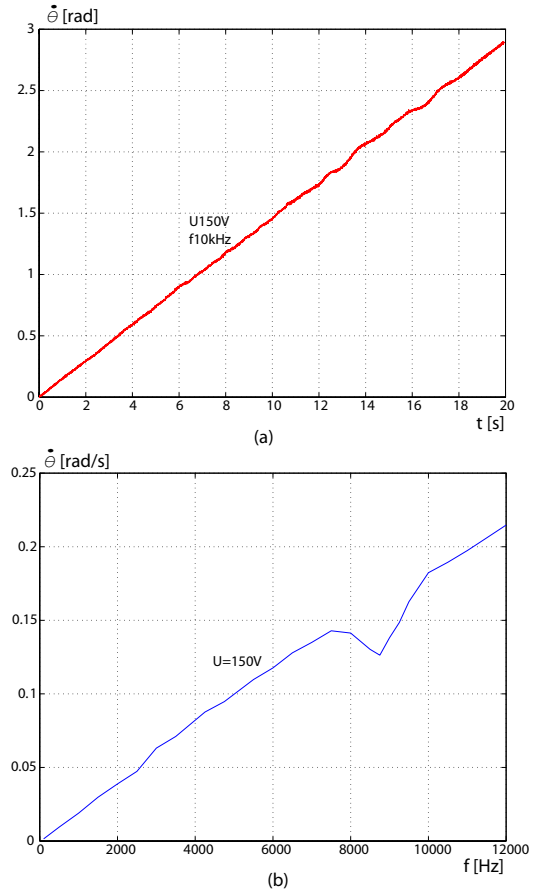


Fig. 13. Characteristic of the angular motion. a : angular displacement of the microsystem for $U = 150V$ and $f = 10kHz$. b : spectrum of the speed for $U = 150V$.

- [4] H. Langen, J.M. Breguet, M. Moscatelli, R. Mericio, Ph. Renaud and H. Bleuler, "Stick-Slip actuators for micromachining of glass" International Conference on Micromechatronics for Information and Precision Equipment, pp-261-264, Tokyo, July, 1997.
- [5] R. Matsuda and R. Kaneko, "Micro-step XY-stage using piezoelectric tube actuator" IEEE Micro Electro Mechanical Systems Conference Proceedings, pp-137-142, 1991.
- [6] O. Fuchiwaki and H. Aoyama, "Design and Control of Versatile Micro Robot for Microscopic Manipulation" Applied Micro Systems, University of Electro-Communications, Tokyo, Japan.
- [7] S.H. Yeo, I.M. Chen, RS Senanayake and P.S. Wong, "Design and development of a planar inchworm robot" School of Mechanical and Production Engineering, Nanyang Technological University, Singapore.
- [8] A. Bergander, W. Driesen, T. Varidel and J.M. Breguet, "Monolithic piezoelectric push-pull actuators for inertial drives," International Symposium Micromechatronics and Human Science IEEE, pp. 309-316, 2003.
- [9] A. Bergander, W. Driesen and J.M. Breguet, "Monolithic piezoelectric actuators for miniature robotic systems" [ACTUATOR, 9th International Conference on New Actuators] 14-16 June 2004, Bremen, Germany.
- [10] M. Rakotondrabe, Y. Haddab, P. Lutz, "Step modelling of a high precision 2DoF (linear-angular) microsystem" Proceedings of the 2005 IEEE International Conference on Robotics and Automation, ICRA, April 2005, Barcelona, Spain.